Proceedings of the 21st ICSMGE, Vienna, Austria, 14 – 19 June 2026. Pistrol, Adam & Schweiger (eds.)
Published by: ÖGG, Austrian Society for Geomechanics, Salzburg, Austria, ISBN 978-3-9503898-4-5
https://doi.org/10.53243/ICSMGE2026-425

Instrumenting and Monitoring a Geosynthetic-Reinforced Pile-Supported MSE Wall Built over Soft Soil

Murad Y. Abu-Farsakh and MohammadAli Izadifar
Louisiana Transportation Research Center, Louisiana State University, Baton Rouge, Louisiana, USA, cefars@lsu.edu

ABSTRACT: The paper will present a case study on instrumenting, monitoring, and finite element modeling (FEM) of geosynthetic-reinforced pile-supported (GRPS) of mechanically stabilized earth (MSE) wall. The GRPS-MSE wall was monitored using various instruments such as piezometers, earth pressure cells, shape-acceleration arrays (SAA), and strain gauges. The performance criteria included efficacy, stress concentration ratio, differential settlement, and reinforcement tension. Collected data, like excess pore-water pressures, contact pressures on pile and soft soil, differential settlements, and lateral displacement of MSE wall, were analyzed thoroughly. A 3D FEM was also developed to simulate the GRPS MSE wall, and the results are in good agreement with field data. The results demonstrated significant load transfer from soil to piles due to soil arching, yielding 30-32 stress concentration ratio (SCR). The field efficacy was measured at 37.69 %, while the FEM efficacy was estimated as 42.4. Strains in geogrids within the GLTP system were under 1%, less than the 5% recommended by FHWA. The horizontal shape-acceleration arrays (SAA) revealed a 12% discrepancy in differential settlement between field and FEM. The MSE wall exhibited low lateral displacement (<25 mm), indicating enhanced stability due to geosynthetic-reinforced load transfer platform (GLTP). The comparison between five analytical GLTP design methods showed that the CUR226 methods gave the closest results to field measurements and FEM results. This study offers crucial insights into leveraging GLTP and MSE walls in highway construction.

KEYWORDS: Geosynthetic-reinforced pile-supported embankment, Geosynthetic load transfer platform, MSE Wall, Analytical design methods, Finite Element Method, Evaluation criteria.

1 INTRODUCTION

Building embankments and other infrastructures over soft subsurface soils often associated with many challenges like possible bearing capacity failure, slope failure, lateral sliding, and excessive differential settlement. One practical approach to this problem is to use geosynthetic-reinforced pile-supported (GRPS) embankments (Van Eekelen et al., 2020). The integration of a load transfer platform (LTP) enables efficient stress redistribution of loads to pile caps and reduction in differential settlement. The transfer of the embankment's vertical load to pile caps is influenced by many factors such as the soil arching, development of geosynthetic tension, and soil-geosynthetic interaction. Understanding the mechanisms of GRPS embankment has been investigated through extensive research, including full-scale field testing (e.g., Cao et al., 2016, Lu et al., 2020), experimental studies (e.g., Rui et al., 2016), and theoretical analyses (e.g., Filz et al., 2019; McGuire et al., 2020). Several studies highlighted the effectiveness of using GRPS embankments in various contexts (e.g., Khansari and Vollmert, 2019; Lee et al., 2019). Their work included embankments on soft subsoil, widened highway embankments, and embankments reinforced with precast high-strength concrete piles or prefabricated vertical drain piles. Several investigators emphasized the importance of performance evaluation, field monitoring, and design considerations in the context of ground improvement for embankments' construction (e.g., Hossain and Rao 2006; Sloan 2011). Their work provided insights into the behavior of various types of embankments, from column-supported to chemico-pile improved, and offered valuable recommendations for their design, construction, and performance assessment.

Despite the extensive research conducted on GRPS embankments, a clear gap emerges in the study of such systems when coupled with Mechanically Stabilized Earth (MSE) walls. This research study not provides critical field data as a benchmark for more advanced analyses of GRPS embankments, and examine important factors like soil arching, load transfer mechanisms, and load-deformation behavior. This could potentially clarify how these integrated systems cooperate to boost overall stability, load-bearing capacity, and settlement reduction, especially under complex construction conditions. This research on integrating the GRPS system with MSE wall case study for the LA 1 Intracoastal Bridge site at Port Allen, Louisiana, offers an opportunity to contribute valuable and innovative insights into the performance and design optimization of such systems. This paper is organized into four sections. The initial part details the description of the current case study of LA 1 Intracoastal Bridge. The subsequent section elucidates the 3D finite element model of this case study. After that, a comparison between the results of the case study and the 3D FEM model is presented, with a detailed examination of the GRPS-MSE wall performance. Lastly, the performance of five GLTP design methods is investigated closely based on field measurements and 3D FEM analysis.

2 SITE DESCRIPTION AND SOIL CONDITIONS

The LA 1 Intracoastal Bridge site at Port Allen, Louisiana was designed using MSE wall supported by GLTP and piles to replace the current bridge with a new bridge constructed on the west side of existing structure. The southbound bridge of LA 1 site consists of three 12-foot lanes and 10-foot shoulders; while the northbound bridge consists of two 12-foot lanes and 10-foot shoulders and a barrier separated exit lane for I-10 eastbound. The MSE wall with 18.5 ft. high was instrumented with 20 ft. long steel straps with cross section = 50 mm × 4 mm. The MSE wall was supported by 1 ft. diameter timber piles of 45 ft. long and 3.5 ft. spacing, and 3.5 ft. geosynthetic LTP on top of piles.

Extensive laboratory and in-situ testing programs were performed to identify the subsurface soil layering and to evaluate the different soil parameters relevant to the project. The subsurface soil condition at LA 1 at the site consists of top 26 ft. of soft lean clay layer (CL), followed by a 10 ft. thick stratum of sand to silty sand, which is underlain by a 8.2 ft. thick clayey silt layer. Below this underlain a 5 ft. thick silty sand layer, which is followed by a 10 ft. thick layer of sandy silt, and then a 13 ft. thick stratum of sand to silty sand. The groundwater table was identified at 1.6 ft. below the surface.

3 INSTRUMENTATION PLAN

A specified section of the GRPS MSE wall at LA 1 Intracoastal Bridge site between pile rows 34 and 39 was selected for

instrumentation and for short-term and long-term monitoring. The selected section was instrumented with multi-level piezometers to monitor the development and dissipation of excess porewater pressure, earth pressure cells to measure the stress transfer, horizontal shape acceleration array (SAA) to measure the settlement profiles below and above the LTP, settlement plates to measure the total settlement of the soil below the GLTP and MSE wall, vertical SAA to measure the lateral displacement of the MSE wall, and strain gages to measure the developed strains along the reinforcements. The configuration and layout of the instrumentation plan at LA 1 site is depicted in three views (cross-section, and plan view) in Figure 1. Photos of field instrumentation of the GRPS MSE wall at LA 1 Intracoastal Bridge site are presented in Figure 1. Selected photos of field instrumentation of the GRPS - MSE wall at LA 1 Bridge site are presented in Figure 2.

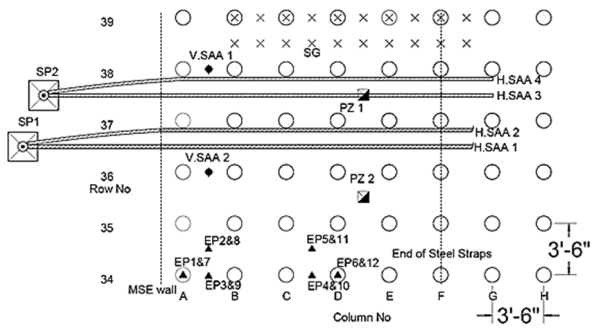

(a) Cross section

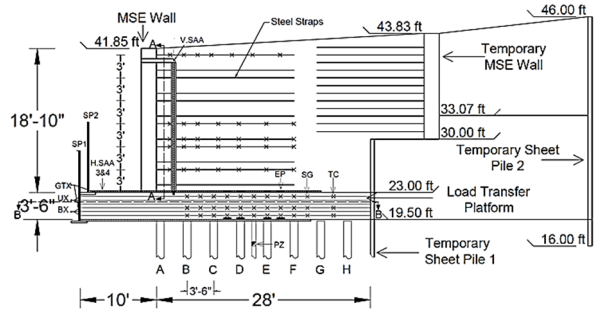

(b) Instrumentation plan (section B-B)

Figure 1. Cross section and Instrumentation plan for LA1 site

Figure 2. Field instrumentation at LA1 site

4 FINITE ELEMENT MODEL

4.1 *Finite element mesh and constitutive modes*

A 3D finite element (FE) model was developed using PLAXIS 3D software to simulate the performance of GRPS - MSE wall system at LA 1 Bridge site. The behavior of non-cohesive soil strata and fill material in MSE wall were represented by the linear elastic perfectly plastic Mohr-Coulomb (MC) model; while the behavior of cohesive soils were characterized using the modified Cam Clay (MCC) model. The pile structures were simulated using the linear elastic (LE) model. The granular fill within the LTP was modeled using the Hardening Soil (HS) model. The input parameters used in soil constitutive models were determined from the results of laboratory and in-situ tests. To ensure accurate numerical results, triangular 10-node elements were selected to generate the FE mesh. Figure 3 depicts the FE mesh used in the 3D model. The lateral boundaries were held fixed in horizontal direction, whereas the bottom boundary was fixed in all directions. To minimize the boundary effect, the finite-element mesh has a horizontal length of 200 ft, equivalent to four times the length of half the GLTP.

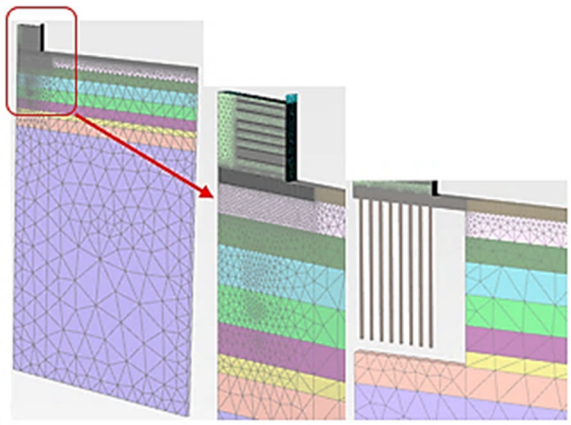

Figure 3. FE mesh for the 3D model.

4.2 *Properties of the geosynthetics-reinforced LTP (GLTP)*

The arrangement of GLTP consists of three biaxial geogrid layers (BXP30) situated underneath three uniaxial geogrid layers (UX1600), all encapsulated within two geotextile layers (Type D GTX) at top and bottom of GLTP. Each layer is separated by a 0.5 ft. spacing, and filled with granular material. The geotextile layers perform the role of separator between the LTP fill material and other soils. Furthermore, they contribute to the load transfer process by bearing tensile forces along their lengths. Figure 1a presents a view of the GLTP configuration. Both the GLTP and MSE wall structures gain support from timber piles (1 ft. diameter and 45 ft. long) arranged in a square pattern with a center-to-center distance of 3.5 ft.

4.3 *Performance Assessment Criteria for GLTP*

Four criteria were used to evaluate the effectiveness of GLTP-MSE wall system: efficacy (E), stress concentration factor (SCR), differential settlement, and maximum tension in geosynthetic reinforcements.

Efficacy (E) is defined as the ratio of total embankment load transferred to piles, providing direct evaluation of the effectiveness of piles in supporting the MSE wall. The stress concentration ratio (SCR) is the ratio of average stress on the pile cap (σ_c) to the average stress on the subgrade soil surface (σ_s) located between the piles. It provides insight into the load transfer mechanism between the piles and subgrade soil. The maximum differential settlement is defined as the difference

between the pile cap's settlement and the settlement at the midspan of the subgrade soil's surface between the piles. The maximum differential settlement between the mid-span of two piles and pile cap can be calculated as (BS8006, 2010):

$$y=(s-a)\sqrt{(3\varepsilon/8)} \quad (1)$$

The following equation can be used to calculate the maximum tension in geosynthetics based on the maximum strain (at pile edge):

$$T=J_{GR}\ \varepsilon \quad (2)$$

where T is the tensile load in geosynthetics, J_{GR} is the axial ultimate tensile stiffness of geosynthetics, and ε is the tensile strain of geosynthetics. According to FHWA (Schaefer et al., 2017), the maximum strain in geogrids should be less than 5%.

5 COMPARISON BETWEEN FEM AND FIELD MEASUREMENTS

5.1 *Excess pore water pressure*

The change in excess pore water pressure (PWP) in this project was not substantial as anticipated, mainly due to the excavation of 7 ft. of embankment at the beginning of construction. Two multi-level piezometers (MLPZs) installed at depths of 20 ft. and 40 ft. were selected to compare the results of FEM with the field measurements, as shown in Figure 4. The figure's declining trend from February 7, 2023, to March 13, 2023, can be attributed to a pause in construction. The fast reduction in excess PWP after completion of construction can be attributed to the arching effect in the GLTP with time that distributes more load on the piles to the deep sandy soil layer.

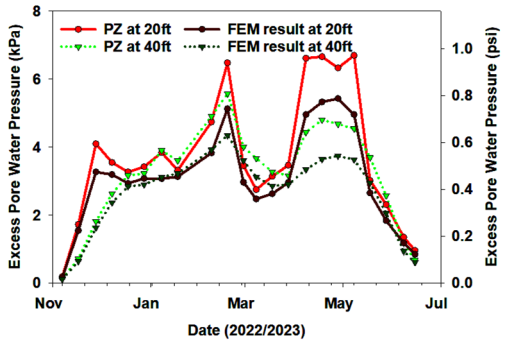

Figure 4. FE computed versus measured excess PWP with time at 20 ft. and 40 ft. depths.

5.2 *Earth pressure efficacy and SCR*

The measurements from earth pressure cells show an increasing trend of vertical pressure over time on top piles, while a decreasing trend of vertical pressure over time on soft soil between the piles, especially below the GLTP (Figures 5a-5d). This variation can be attributed to the arching effect phenomenon. As the soil consolidates and the system settles over time, a larger proportion of MSE load is transferred to the pile tops as compared to that between the piles.

The distinct difference in vertical stress values above and below the GLTP is obvious. The pressure beneath the GLTP (EP1 to EP6) is notably higher, specifically for EP cells positioned on top of piles. Below the GLTP, the pressure exerted on top of piles to about 800 kPa; while above the GLTP (EP7 to EP12), the pressure on top of piles is about 20-40 kPa. These measurements highlight the significant soil arching that occurs when the GLTP is used, which effectively redistributes the MSE load to the top of piles. The results of 3D FEM analysis effectively depict this soil arching, as shown in Figure 5e.

The efficacy and SCR ratio can be determined from measurements of the earth pressure cells and FEM results. The field efficacy is calculated to be 37.69%, while the FEM results indicate 42.4% efficacy, resulting in a 12% disparity between the field and FEM analysis. For SCR, the field data gives a range between 30 and 32; while the FEM analysis reveals a value of 31, a 3% discrepancy between field and FEM results.

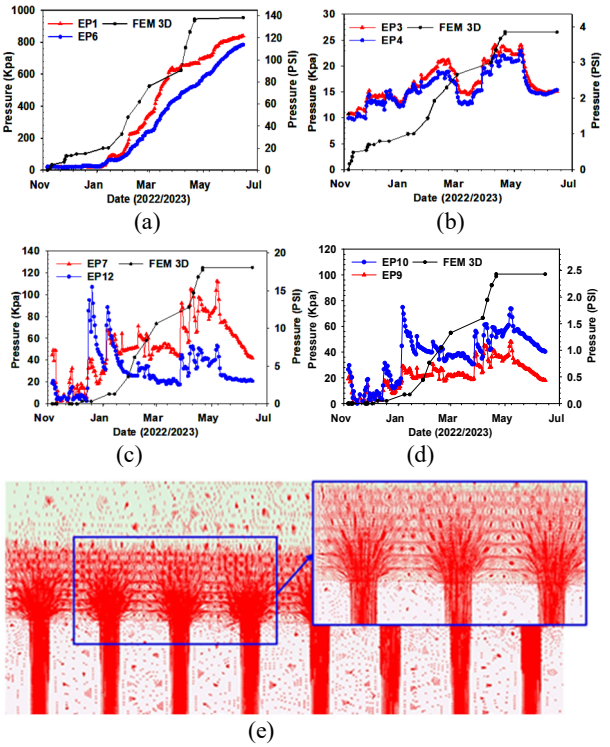

Figure 5. Pressure values with time from EP cells: (a) below GLTP on top of pile head; (b) below GLTP on soil between piles'; (c) above GLTP on top of pile head; (d) above GLTP on soil between piles' straight spacing; and (e) total principal stresses derived from FEM 3D model with arching.

5.3 *Results of SAAs and differential Settlement*

Four horizontal SAAs attached to two "reference" settlement plates were installed to measure the total settlement above and below the GLPT. Measurements from the settlement plates were used to adjust the SAAs measurements at the end to determine the profiles of total settlements with time under the MSE wall, as shown in Figure 6. The settlement profiles obtained from 3D FEM were compared with the measured settlement profiles from SAAs. The results of 3D FEM analysis align closely with the field SAA measurements. The differential settlement between the soft soil and piles over time above and below the GLTP was tracked comparing the results of horizontal SAAs located adjacent to the piles with those installed on soil at mid distance between the piles. The maximum differential settlement recorded from the difference of horizontal SAA1 & SAA2 stands at 7.1 mm, while the maximum differential settlement yielded from the FEM analysis is 8.3 mm.

5.4 *Lateral displacement of MSE wall*

The lateral displacement of MSE wall can provide insights into stability and serviceability of the wall. The lateral displacement of MSE wall at LA 1 Bridge site was measured using two vertical SAAs, and the results are presented in Figure 7a. The figure also includes the results of 3D FEM analysis, which shows the magnitude and bulging profile close to SAA2

measurements. The contours of lateral displacement from FEM are presented in Figure 7b. The performance of MSE wall shows an increase in the lateral displacement of the MSE wall with height up to 12 to 14 ft., which then decreases in higher levels of the wall. The maximum lateral displacement measured from VSAA2 is about 25 mm at about 14 ft. height from the toe; whereas the estimated maximum displacement from 3D FEM is about 23 mm that occurs at about 12 ft. According to FHWA design guideline (Christopher, 1990) for inextensible reinforcement, the maximum lateral displacement should be < ¾ in. for every 10 ft. of wall height. This translates into a lateral displacement of 1.39 in. (35.24 mm). Both the field and FEM values of maximum lateral displacement are lower than this limit.

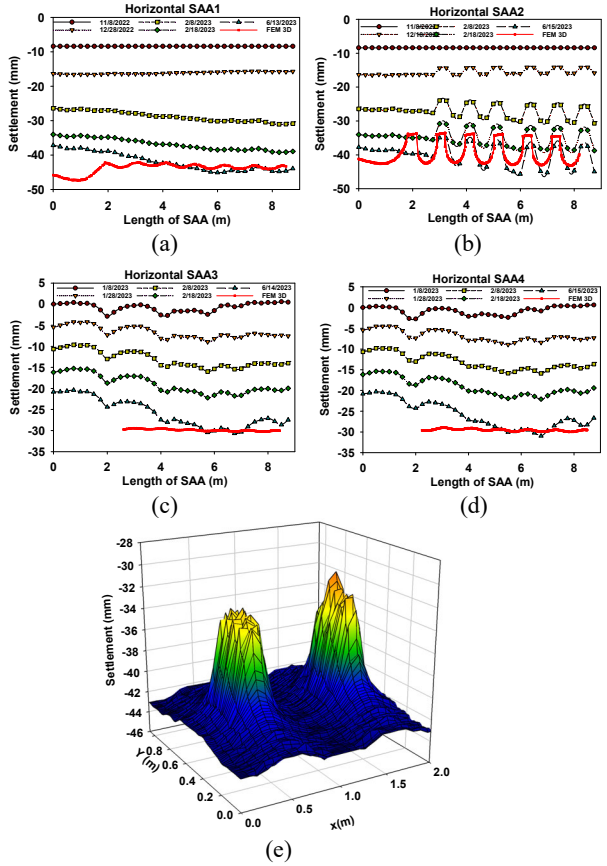

Figure 6. Settlement profiles of instrumented section: a) SAA1; b) SAA2; c) SAA3; d) and SAA4.

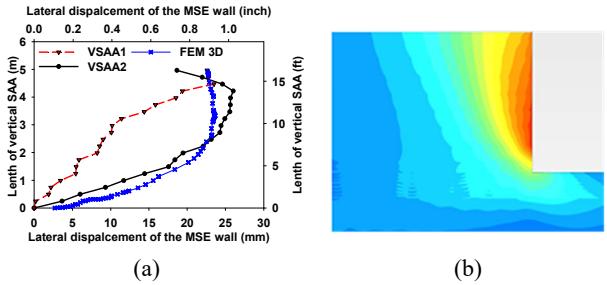

Figure 7. Lateral displacement of MSE wall: a) Comparison between field measurements and 3D FEM; b) Contours of lateral displacement from 3D FEM.

5.5 *Distribution and maximum strains along geosynthetics*

Vibrating wire strain gauges were installed along 2 biaxial geogrid layers and one uniaxial geogrid layer to measure the distribution of strains along geosynthetics. The distribution of strain obtained from strain gauges, as well as those obtained from 3D FEM analysis are presented in Figures 8a, 8b, and 8c, for the 2nd biaxial geogrid layer, 4th biaxial geogrid layer, and 6th uniaxial geogrid layer, respectively. A maximum strain of about 0.7% was observed for the 2nd geogrid layer. The decrease in strain values in uniaxial geogrid as compared to biaxial geogrid can be attributed to its higher modulus of elasticity. The strain distribution across all geosynthetic layers exhibited a characteristic peak-trough pattern.

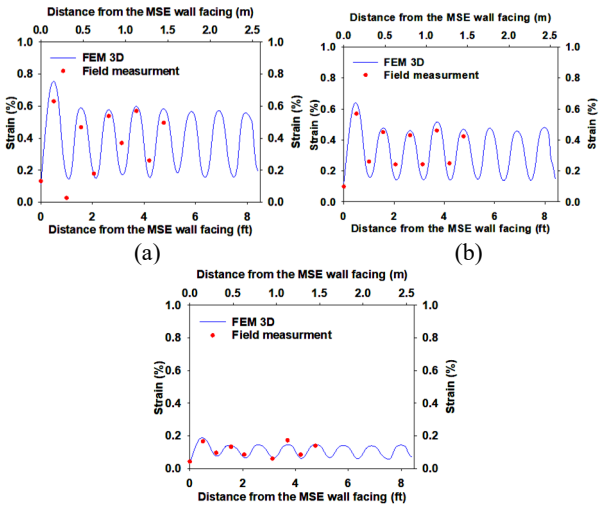

Figure 8. Strain distribution along: a) 2nd biaxial geogrid layer; b) 4th biaxial geogrid layer; and c) 6th uniaxial geogrid layer.

As shown in Figure 8, all measured strains fall below 1%, significantly lower than the maximum strain limit of 5%, as recommended by FWHA. This suggests that the design manual for GLTP might be conservative that could be revised for more cost-effective designs.

6 COMPARISON WITH GLTP DESIGN METHODS

Several analytical methods were proposed in literature for design of GRPS embankments, and this study will examine five of them using field measurements and 3D FE results. These methods include the British (BS8006, 2010), German (EBGEO, 2011), Nordic (NGG, 2005), Dutch (CUR226, 2016), and the FHWA (Schaefer et al., 2017) methods. A very brief description of each method will be given below. For more comprehensive details of these methods, the reader can refer to Izadifar et al. (2023), or in the corresponding reference of each method.

The British standard, BS8006 (2016), employs the method developed by Hewlett and Randolph (1988) to evaluate the vertical load on geosynthetic reinforcement. It emphasizes the least effective arching between the crown and pile cap areas but overlooks subsoil support.

The German standard, EBGEO (2011) applies the method introduced by Kempfert et al. (2004). It incorporates the multi-arching theory and lower bound theorem from plasticity theory to assess the vertical stresses. It considers the subsoil support when determining the reinforcement tension. The EBGEO design code provides charts for estimating the maximum strain.

The Dutch standard, CUR226 (2016), utilizes the concentric arches model proposed by Van Eekelen et al. (2013). It splits the vertical load into three elements: the load on pile cap, the load on square area of geosynthetic reinforcement distributed within 3D hemisphere, and load on the geosynthetic reinforcement strips formed from 2D arches.

The FHWA (Schaefer et al., 2017) design manual details a design process for GRPS embankments, employing the load-displacement compatibility method proposed by Filz and Smith (2006). It subdivides the vertical load into four sections, with the system's vertical equilibrium achieved when the total downward force matches the total upward force. It provides numerous formulas to calculate the vertical load atop the pile cap and geosynthetic reinforcement, depending on the embankment's critical height. Geosynthetic tension is calculated using the parabolic method.

The Nordic Design Guideline (NGG, 2005) takes a different approach by estimating the load borne by reinforcement based on a soil wedge assumption rather than direct calculation of arching and vertical load. It determines the soil's weight in three dimensions and the vertical stress on top of subgrade, yielding formulas for calculating reinforcement tension.

The performance of the five analytical methods for designing GRPS were evaluated using four different criteria: efficacy, stress concentration ratio (SCR), maximum tension in geosynthetics, and differential settlement between pile cap and soil. The comparison between the five design methods, 3D FEM, and the field measurements are presented in Figure 9. The figure demonstrates notable distinctions in the prediction capabilities of the different design methods concerning efficacy, geosynthetic tension, and differential settlement. The 3D FEM and the CUR 226 analytical approach offer more precise estimation of these criteria as compared to alternative design techniques. Subsequently, both the EBGEO and FHWA design methodologies prove effective in forecasting arching and geosynthetic tension. However, they tend to overestimate the differential settlement. The limit equilibrium model, which is used in CUR226, EBGEO, and FHWA, emerges as a robust and high-performing method. Furthermore, analytical techniques that incorporate the influence of subsoil support, the CUR226 and EBGEO methods, align more closely with experimental findings than those neglect this factor. The pronounced overestimation observed in the BS8006 design guideline relative to other standards can be attributed to its exclusion of subsoil support effects. Overall, it can be concluded that the BS8006 and Nordic design methodologies are the least accurate that tend to produce conservative results.

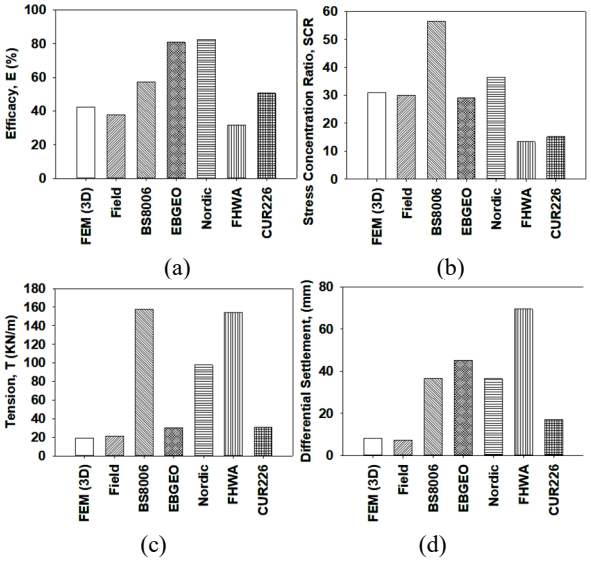

Figure 9. Evaluation of GRPS design methods and FEM based on field measurements using four criteria: a) Efficacy, b) SCR, c) Tension in geosynthetics, and d) Differential Settlement between pile cap and soil.

7 CONCLUSIONS

Based on the findings of this study, the following conclusions can be drawn:

- The results of FEM are in good agreement with the field measurements, in terms of excess pore water pressure, settlement, pressure distribution, strain distribution along reinforcements, and lateral displacement of MSE wall.
- The results demonstrated significant load transfer from the soil to piles caused by soil arching, resulting in SCR of 30-32. The SCR from FEM is 31. The field efficacy was measured at 37.69%, while the FEM efficacy was estimated at 42.4%. CUR226 and EBGEO yield predictions of 17.3% and 29% for the SCR, respectively.
- The maximum differential settlement measured between pile cap and soil from SAAs is 7.1 mm, and 8.3 mm from FEM is. CUR226 estimates the maximum differential settlement at 17 mm. This estimation aligns closely with empirical field observations and FEM outcomes.
- The measured and FEM estimated of strain values on geosynthetics are <1%, significantly lower than the 5% recommended by the FWHA.
- The MSE wall exhibited low lateral displacement (<25 mm), indicating enhanced stability due to use of GRPS and steel straps. The maximum strains on steel straps are 1% and 1.5% from field and FEM, respectively.
- The maximum tension in geosynthetics measured from field is 21.3 kN/m and 19.2 kN/m from FEM. Outcomes from analytical design also show that CUR226 and EBGEO outperform the other guidelines by predicting maximum tension of 31 kN/m and 29 kN/m, respectively.
- The CUR226 method aligns well with empirical field and FEM outcomes regarding efficiency criteria, yielding results of 50.5, 38, and 42, respectively.
- Overall, CUR226 demonstrated the most accurate design method for estimating the four design criteria, with the FHWA and EGBEO methods also delivering good estimates in several criteria.

8 ACKNOWLEDGMENTS

This research is funded by the Louisiana Transportation Research Center (Project No. 20-2GT) and Louisiana Department of Transportation and Development (LA DOTD) (Project No. DOTLT1000337). The authors would like to thank LA DOTD engineers for providing valuable help and support.

9 REFERENCES

BS 8006-1, 2010. Code of Practice for Strengthened/reinforced Soils and Other Fills. British Standards Institution BSI, London, UK.

Cao, W.Z., Zheng, J.J., Zhang, J., and Zhang, R.J., 2016. Field Test of a Geogrid-Reinforced and Floating Pile-Supported Embankment. Geosynthetics International, 23: 348–361.

Christopher, B. R., 1990. Reinforced Soil Structures, Vol. I: Design and Construction. Federal Highway Administration Report No. FHWA-RD-89-043.

CUR 226, 2016. Design Guideline Basal Reinforced Piled Embankments. In: Design Guideline Basal Reinforced Piled Embankments. CRC press.

EBGEO, 2011. Recommendations for Design and Analysis of Earth Structures Using Geosynthetic Reinforcements. Digital in English. German geotechnical society.

Filz, G. and Smith, M., 2006. Design of Bridging Layers in Geosynthetic-reinforced Column-supported Embankments. Virginia Transportation Research Council, Charlottesville, Virginia.

Filz, G.M., Sloan, J.A., McGuire, M.P., Smith, M., and Collin, J. Settlement and Vertical Load Transfer in Column-Supported

Embankments. Journal of Geotechnical and Geoenvironmental Engineering, 2019. 04019083.
Hewlett, W.J., and Randolph, M.F., 1988. Analysis of Piled Embankments. International Journal of Rock Mechanics and Mining Sciences & Geomechanics Abstracts, 25: 297–298.
Hossain, S., Rao, K.N., 2006. Performance Evaluation and Numerical Modeling of Embankment Over Soft Clayey Soil Improved with Chemico-Pile. Transportation Research Record, 1952(1): 80–89.
Izadifar, M., Luo, N., Abu-Farsakh, M. Y., Chen, S., 2023. Performance Evaluation of Design Methods for Geosynthetic-reinforced Pile-supported Embankments. Transportation Research Record, Vol. 2677, Issue 11.
Kempfert, H.G., Gobel, C., Alexiew, D., and Heitz, C., 2004. German Recommendations for Soil Reinforcement above Pile-Elements. In: EUROGeo3, Third Geosynthetic Conference, Munchen, Vol. 1, pp. 279–283.
Khansari, A., Vollmert, L., 2019. Load Transfer and Deformation of Geogrid-Reinforced Piled Embankments: Field Measurement. Geosynthetics International, 1–10.
Lee, T., Lee, S.H., Lee, I.W., Jung, Y.H., 2019. Quantitative Performance Evaluation of GRPE: A Full-Scale Modeling Approach. Geosynthetics International, 1–6.
Lu, W., Miao, L., Wang, F., Zhang, J., Zhang, Y., and Wang, H. 2020. A Case Study on Geogrid-Reinforced and Pile-Supported Widened Highway Embankment. Geosynthetics International, 27: 261-274.
McGuire, M., Sloan, J., and Filz, G., 2020. Effectiveness of Geosynthetic Reinforcement for Load Transfer in Column-Supported Embankments. Geosynthetics International, 27: 200–218.
NGG (Nordic Geosynthetic Group), 2005. Nordic Guidelines for Reinforced Soils and Fills.
Rui, R., van Tol, F., Xia, X.L., van Eekelen, S., Hu, G., and Xia, Y.Y. 2016. Evolution of Soil Arching; 2D DEM Simulations. Computers and Geotechnics, 73: 199–209.
Schaefer, V. R., Berg, R. R., Collin, J. G., Christopher, B. R., DiMaggio, J. A., Filz, G. M., and Ayala, D., 2017. Ground Improvement Methods–Reference Manual Vols. I and II. FHWA-NHI-16-027 and FHWA-NHI-16-028.
Sloan, J.A. 2011. Column-supported Embankments: Full-scale Tests and Design Recommendations. Doctoral dissertation, Virginia Tech, Blacksburg, VA.
Van Eekelen, S.J.M., Bezuijen, A., and Van Tol, A.F., 2013. An Analytical Model for Arching in Piled Embankments. Geotextiles and Geomembranes, 39: 78–102.
Van Eekelen, S.J.M. and Han, J., 2020. Geosynthetic-Reinforced Pile-Supported Embankments: State of The Art. Geosynthetics International, 27(2): 112–141.